ACS APPLIED MATERIALS & INTERFACES

Research Article

www.acsami.org

PLLA Nanofibrous Paper-Based Plasmonic Substrate with Tailored Hydrophilicity for Focusing SERS Detection

Jundong Shao,[†,‡,§,∥] Liping Tong,[‡,∥] Siying Tang,[‡] Zhinan Guo,[†,‡] Han Zhang,*[,†] Penghui Li,[‡] Huaiyu Wang,[‡] Chang Du,*[,§] and Xue-Feng Yu*[,‡]

[†]SZU-NUS Collaborative Innovation Center for Optoelectronic Science and Technology, and Key Laboratory of Optoelectronic Devices and Systems of Ministry of Education and Guangdong Province, College of Optoelectronic Engineering, Shenzhen University, Shenzhen 518060, P.R. China

[‡]Institute of Biomedicine and Biotechnology, Shenzhen Institutes of Advanced Technology, Chinese Academy of Sciences, Shenzhen 518055, P.R. China

[§]National Engineering Research Center for Tissue Restoration and Reconstruction, South China University of Technology, Guangzhou 510006, P.R. China

Supporting Information

ABSTRACT: We report a new paper-based surface enhanced Raman scattering (SERS) substrate platform contributed by a poly(L-lactic acid) (PLLA) nanofibrous paper adsorbed with plasmonic nanostructures, which can circumvent many challenges of the existing SERS substrates. This PLLA nanofibrous paper has three-dimensional porous structure, extremely clean surface with good hydrophobicity (contact angle is as high as 133.4°), and negligible background interference under Raman laser excitation. Due to the strong electrostatic interaction between PLLA nanofiber and cetyltrimethylammonium bromide (CTAB) molecules, the CTAB-coated gold nanorods (GNRs) are efficiently immobilized onto the fibers. Such a hydrophobic paper substrate with locally hydrophilic SERS-active area can confine analyte molecules and prevent the random spreading of molecules. The confinement leads to focusing effect and the GNRs-PLLA SERS substrate is found to be highly sensitive (0.1 nM Rhodamine 6G and malachite green) and exhibit excellent reproducibility (~8% relative standard deviation (RSD)) and long-term stability. Furthermore, it is also cost-efficient, with simple fabrication methodology, and demonstrates high sample collection efficiency. All of these benefits ensure that this GNRs-PLLA substrate is a really perfect choice for a variety of SERS applications.

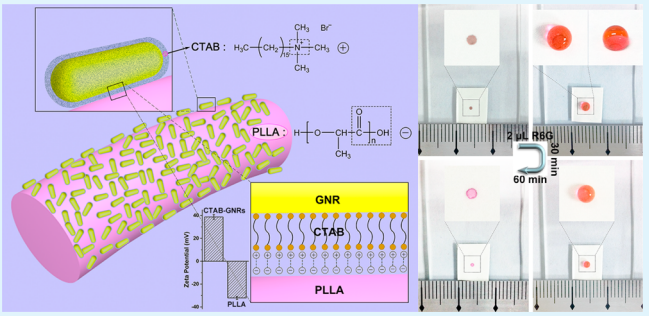

KEYWORDS: *PLLA nanofibrous paper, surface-enhanced Raman spectroscopy, gold nanorods, hydrophobic, plasmonic*

1. INTRODUCTION

Surface enhanced Raman scattering (SERS) has been regarded as one of the most powerful spectroscopic techniques for label-free detection of various chemical and biological species because of its capability to provide a spectroscopic fingerprint of each molecule.[1,2] Ultrasensitive analysis can be achieved with SERS owing to the electromagnetic and chemical enhancement mechanism of noble metal nanostructures,[3,4] whereas the application of SERS in molecule analysis is largely hindered by problems mainly associated with the reproducibility and complexity in substrate preparations.[5] So far, many different techniques, such as physical vapor deposition,[6,7] electron beam lithography,[8−10] colloidal lithography,[11,12] nanosphere lithography[13,14] and other strategies,[15,16] are currently available for the fabrication of well-ordered periodic silver or gold nanoparticle arrays, which enable precise control over the shape, size, and organization of the metal nanostructures.[17] SERS substrates obtained by these techniques show a large Raman enhancement ability and good SERS reproducibility, which enables SERS as a single-molecule detection technique to identify analytes at trace levels.[18] These substrates exhibit excellent SERS performances for various ultrasensitive analyses in laboratory.

On the other hand, much recent attention has been paid toward the paper-based SERS substrates for on-site analytical applications in the real world.[19−29] Because paper is inexpensive, flexible, and lightweight and can wick the samples by capillary forces, the paper-based SERS substrates showed advantages in SERS performance, cost, reproducibility, and instrument independence and they could be fabricated immediately before sample analysis.[30] A great deal of researches have been carried out to impregnate plasmonic nanoparticles

Received: December 16, 2014
Accepted: February 20, 2015
Published: February 20, 2015

DOI: 10.1021/am508881k
ACS Appl. Mater. Interfaces 2015, 7, 5391−5399

into various papers such as filter paper,[22−25] photocopy paper,[27,28] and cellulose paper,[29] etc. For instance, Singamaneni et al. reported the filter-paper-based substrates by dip-coating gold nanorods (GNRs) into filter paper.[24] Liz-Marzán et al. developed a pen-on-paper approach to fabricate SERS substrates with A4 photocopy paper.[27] However, these papers are generally not clean enough, which produces high background interference in the SERS detection. Furthermore, their hydrophilic surface property may led to the spread of the sample over the paper by capillarity, which made it difficult to concentrate the analyte molecules at a SERS-active area for a higher efficiency.[31,32] Another example in this area is the work by Yu et al., who reported the preparation of arrays of SERS active sites on hydrophobized cellulose paper by printing silver nanoparticles using an inkjet printer.[29] The hydrophobic surface of this paper enabled the concentration of analyte to the SERS sensing pattern. However, specific instrumentation is indispensable in this process.

Poly(L-lactic acid) (PLLA), as one of the most prominent biodegradable and biocompatible polymers, has attracted much attention from the academic viewpoint as well as the practical applications.[33,34] PLLA is derived from 100% renewable resources such as corn starch, chips, or sugar cane and could be eventually degraded into CO_2 and H_2O under natural conditions.[35] As an excellent environmentally friendly material, PLLA is now widely used in commodity applications, tissue engineering, and regenerative medicine. In particular, PLLA nanofibrous papers prepared by electrospinning technique with a high porosity and a large surface area have been proven to be ideal for applications in tissue engineering and regenerative medicine.[36] Apart from the excellent biodegradability and biocompatibility, electrospinning PLLA papers with three-dimensional (3D) nanofibrous structure, relatively simple and stable chain conformation, and strong hydrophobicity can be expected to be an ideal SERS substrate.

Herein, we present the fabrication of a new paper-based SERS substrate contributed by a hydrophobic nanofibrous PLLA paper synthesized by electrospinning. Due to the strong electrostatic interaction between PLLA nanofiber and cetyltrimethylammonium bromide (CTAB) molecules, the CTAB-coated GNRs can be efficiently immobilized onto the hydrophobic PLLA nanofibrous paper, resulting in locally hydrophilic hot-spot areas. The obtained GNRs-PLLA paper demonstrates a hydrophobic−hydrophilic focusing effect and can serve as a SERS substrate with negligible background interference, high sensitivity, good reproducibility, and excellent long-term stability.

2. MATERIALS AND METHODS

2.1. Materials and Reagents. Chemicals used in GNRs synthesis such as $HAuCl_4{\cdot}3H_2O$, $NaBH_4$, and CTAB were obtained from Sigma-Aldrich (St. Louis, MO). Silver nitrate ($AgNO_3$) and ascorbic acid were purchased from Sinopharm Chemical Reagent Co. Ltd. (Shanghai, China). PLLA with an inherent viscosity of 1.46 dL/g was purchased from DaiGang Biomaterial Co. Ltd. (Shandong, China). *N*,*N*-Dimethylformamide (DMF) and dichloromethane (DCM) were obtained from Beijing Chemical Co. (Beijing, China). Deionized water was obtained with a Milli-Q water filter system from Millipore Corporation (France). All reagents were used directly without further purification.

2.2. Synthesis of GNRs. The GNRs were synthesized in an aqueous solution via a seed-mediated growth method by using CTAB as the surfactant, and the detailed procedures have been reported previously.[37] In brief, the 3−4 nm gold seed particles were prepared by mixing 5 mL of 0.5 mM $HAuCl_4$ with 5 mL of 0.2 M CTAB. The solution was stirred vigorously followed by dropwise addition of 600 μL of freshly prepared ice-cold 10 mM of $NaBH_4$. The reaction was then left undisturbed for more than 2 h to ensure complete Au^{3+} reduction. In the GNRs synthesis, 18 mL of 5 mM $HAuCl_4$ and 225 μL of 0.1 M $AgNO_3$ were added to 90 mL of 0.2 M CTAB and then 200 μL of 1.2 M HCl and 10.5 mL of 10 mM ascorbic acid were added and gently swirled to change the color from dark orange to colorless. Afterward, 120 μL of the CTAB-stabilized gold seed solution was rapidly injected. The obtained solution was gently mixed for 10 s and left undisturbed overnight. Finally, the GNRs solution was centrifuged at 10000 rpm for 10 min to stop the reaction. The supernatant was removed, and the precipitate was resuspended in ultrapure water. The GNR concentration was estimated to be about 0.65 nM according to the extinction coefficient at longitudinal surface plasmon resonance (LSPR) wavelength.[38]

2.3. Preparation of PLLA Nanofibrous Paper-Based SERS Substrates. PLLA nanofibrous papers were fabricated by electrospinning according to the procedures reported by Chen et al.[39] In brief, a 10% (w/v) homogeneous polymer solution was prepared by dissolving PLLA in a 4:1 mixture of DCM and DMF by gentle rocking at room temperature for 12 h. The polymer solution was placed into a syringe with a stainless steel needle (inner diameter of 0.6 mm) and pumped continuously at a rate of 1 mL/h. The distance between the needle tip and the surface of the collecting drum (covered with aluminum foil) was 15 cm. During electrospinning, a high voltage power supply was used to apply a 20 kV potential difference between the tip and the grounded collector. After electrospinning for 1 h, the obtained PLLA nanofibrous paper was then placed in a vacuum desiccator overnight to remove residual solvent. Finally, the GNRs aforementioned were dropped onto the PLLA nanofibrous paper by a glass spotting capillary tube (inner diameter of 0.3 mm) to prepare SERS substrates.

2.4. Characterizations. Transmission electron microscopy (TEM) images were acquired on a JEOL JEM-2010 transmission electron microscope operating at an accelerating voltage of 200 kV. Absorption spectra were taken on a TU-1810 UV−vis spectrophotometer (Purkinje General Instrument Co. Ltd. Beijing, China). The morphology of PLLA nanofibrous paper and SERS substrates based on it were observed by scanning electron microscopy (NOVA NANO-SEM430, FEI, The Netherlands) at 5−10 kV after gold coating for 120 s with a sputter coater (EM-SCD500, Leica, Germany). The hydrophilicity/hydrophobicity of samples was evaluated by employing static contact angle measurements with the sessile drop method using an OCA20LHT-TEC700-HTFC1500 (Dataphysics, Germany) contact angle goniometer. The ζ potential was determined by the Zetasizer Nano ZS (Malvern Instruments Ltd., UK) at 25 °C. Raman scattering was performed on a Horiba Jobin-Yvon LabRam HR VIS high-resolution confocal Raman microscope equipped with a 633 nm laser as the excitation source at room temperature.

3. RESULTS AND DISCUSSION

A three-dimensional PLLA nanofibrous paper was employed as the paper scaffold to load with the plasmonic nanostructures for enabling SERS. The PLLA nanofibrous paper was synthesized by using electrospinning technology, which was a well-known facile electrohydrodynamic method to fabricate various solid nanofibers with high purity and high yield.[40] In this work, the synthesized PLLA nanofibrous paper has a smooth and uniform surface and their size can be as large as 13 × 30 cm^2 (see Figure 1a). Furthermore, the PLLA nanofibrous paper can be free-standing with good flexibility (see inset in Figure 1a). To evaluate its hydrophilicity/hydrophobicity, the contact angle of a water droplet on the PLLA nanofibrous paper was measured by using the sessile drop method (see Figure 1b). The water contact angle was as high as 133.4°, demonstrating the good hydrophobicity of the PLLA nanofibrous paper, which was mainly owing to the possible surface segregation of hydro-

DOI: 10.1021/am508881k
ACS Appl. Mater. Interfaces 2015, 7, 5391−5399

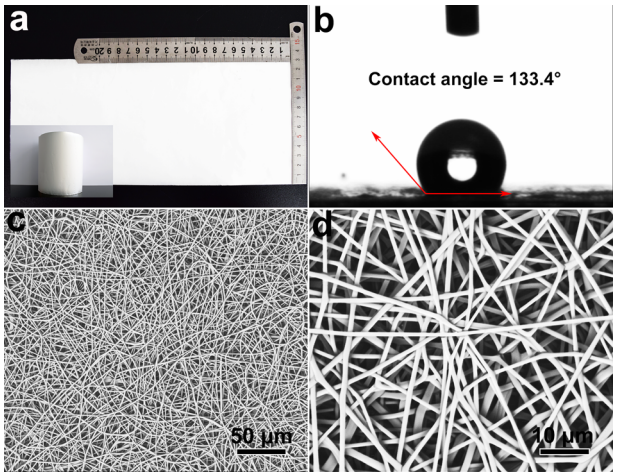

Figure 1. (a) Photographs, (b) contact angle measurement, and (c) low-magnification and (d) high-magnification SEM images of PLLA nanofibrous paper prepared via electrospinning.

phobic methyl groups and the porous surface morphology with nanofibrous architecture.[41] The surface topography of PLLA nanofibrous paper was determined by SEM, and the images are shown in Figure 1c,d. It was clear that a three-dimensional uniform PLLA nanofibrous network with high porosity was formed and the diameter of the fibers was varied from 500 to 800 nm.

The GNRs were used as the typical plasmonic nanostructures for SERS applications owing to the facile tunability of longitudinal SPR (to fit to the source laser) and sharp corners (to obtain efficient electromagnetic hot spots).[42−49] Figure 2a reveals that the average diameter and length of the GNRs are 13 ± 2 and 43 ± 3 nm, respectively. As shown in Figure 2b,

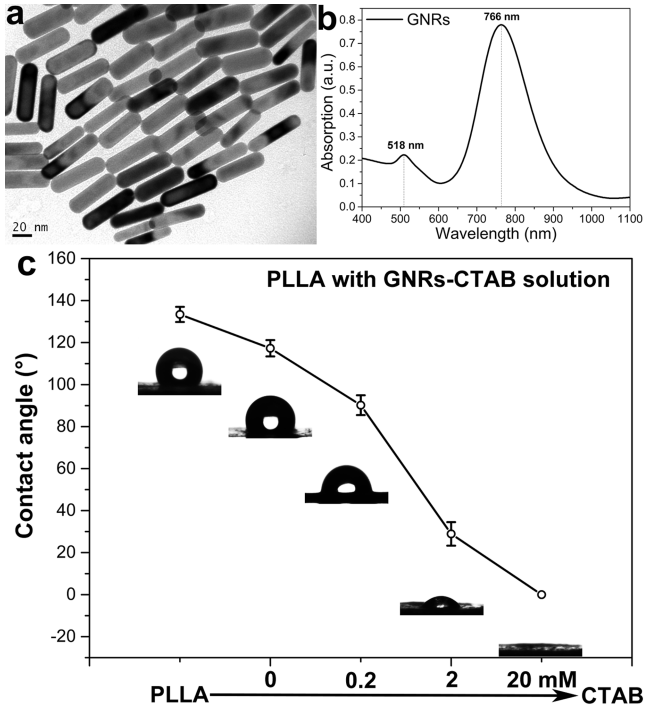

Figure 2. (a) TEM image and (b) absorption spectra of GNRs. (c) Contact angle measurements of PLLA nanofibrous paper after dropping GNRs-CTAB solution with increased CTAB concentration.

there were two characteristic peaks at ~518 and ~766 nm in the extinction spectra of the GNRs solution corresponding to the transverse SPR band and longitudinal SPR band of the GNRs, respectively.[22] It should be emphasized that the GNRs were synthesized by using a well-known seed-mediated growth method with CTAB as the capping agent, and the GNRs could be stabilized in CTAB solution for long-term preservation.[37]

Interestingly, it was found that the GNRs solution could be used to tailor the hydrophilicity of the PLLA nanofibrous paper. As shown in Figure 2c, when the GNRs solution was dropped onto the PLLA nanofibrous paper, the contact angle of the paper decreased from 133.4° to 0° with the increase of CTAB concentration. The results suggested that the hydrophilic spots could be obtained in such hydrophobic paper just by dropping the GNRs solution onto their surface.

A schematic illustration is shown in Figure 3 to demonstrate the possible interaction between CTAB and PLLA nanofiber.

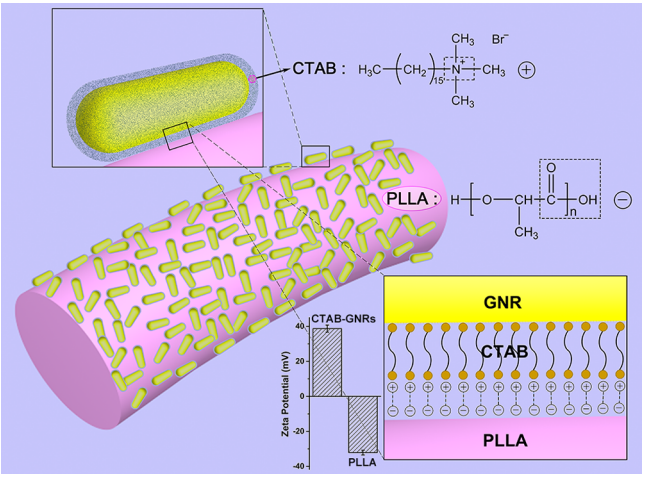

Figure 3. Schematic illustration of the interaction mechanism between CTAB and PLLA nanofiber.

For the GNRs, the capping CTAB molecules form a partially interdigitated bilayer on the surface of GNRs. The GNR surface was considered to be negatively charged due to the adsorption of chloride or bromide ions, while the ammonium head groups in CTAB carry positive charges. Through electrostatic interaction, the ammonium head groups in CTAB bond tightly to the GNR surface to form the inner layer. Another layer of CTAB molecules was assembled because the hydrophobic carbon-chain tail of CTAB could interact with the inner layer and the ammonium groups point outside.[50] The CTAB bilayer made the GNRs positively charged[51] with the ζ potential of about 38.7 ± 2.02 mV. For the PLLA nanofibrous paper, the surface of PLLA nanofibers was believed to be negatively charged owing to the −COOR groups of PLLA.[52] Correspondingly, the ζ potential of the PLLA nanofibrous paper was about −32.1 ± 1.36 mV, and the strong electrostatic interaction between CTAB and PLLA nanofiber enabled the efficient binding of GNRs onto the PLLA nanofibrous paper.

The aforementioned results demonstrated a strategy to prepare the GNRs-PLLA paper substrate with hydrophilic plasmonic hot-spot (SERS active area) on the hydrophobic PLLA nanofibrous paper. To minimize the area of the hot-spot, only 0.1 μL of the GNRs-CTAB solution was dropped onto the PLLA nanofibrous paper by using a glass spotting capillary tube with an inner diameter about 0.3 mm. As shown in Figure 4a,

DOI: 10.1021/am508881k
ACS Appl. Mater. Interfaces 2015, 7, 5391−5399

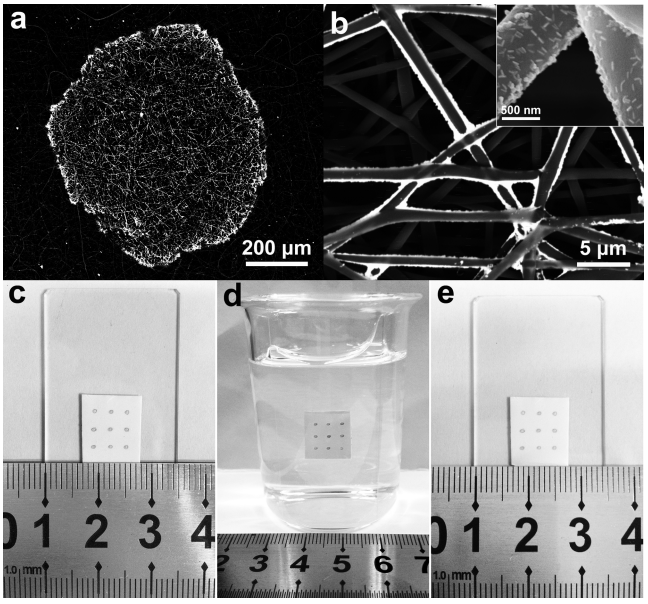

Figure 4. (a,b) SEM images of one typical plasmonic hot-spot (a) and its detailed structures (b). Inset graph in (b) is a higher magnification SEM image. (c–e) Photographs of a GNRs-PLLA array (c) which was dipped into water for 15 min (d) and then extracted and dried (e).

the achieved hot-spot was in ring-like shape due to the known "coffee-ring effect"[53] with a diameter of only 700 μm. Figure 4b revealed the detailed SEM images of the SERS active area. It could be observed that the GNRs were tightly bound onto the PLLA nanofibers instead of being deposited on the paper surface. Furthermore, compared to the two-dimensional planar substrates, such three-dimensional nanofibrous paper substrates with hierarchical structure provided the increased surface area and enhanced absorption capacity for easy access of analytes.[54] Just by dropping the GNRs-CTAB solution one by one, a SERS array with 3 × 3 hot-spots on a piece of 1 × 1 cm^2 PLLA nanofibrous paper could be easily fabricated (see Figure 4c). Figure 4d,e demonstrated the stability of the GNRs-PLLA paper substrate, which was indicated by the invariance of the patterns after dipping in water and subsequent drying. In fact, only 0.8% amount of the GNRs was detached from the substrates with a 15 min dipping process by testing the absorption spectra of the cleaning water before and after substrate dipping (data not shown). The good stability of the GNRs-PLLA paper substrate in water was ascribed to the strong electrostatic interactions between PLLA and CTAB molecules.

The background interference of the substrate could hinder the SERS performance, but generally it was neglected. Here in this study, the background interference of the GNRs-PLLA paper under Raman laser excitation was examined and compared to the GNRs-filter-paper (see Figure 5). It was well-recognized that the filter paper was mainly composed of α-cellulose[55] (98% cotton fiber), of which the background interference was very small. However, when the GNRs was dropped onto the filter paper, strong Raman signals could be observed in such GNRs-filter-paper even after the baseline correction. In contrast, the GNRs-PLLA paper exhibited very faint Raman signals, for which the baseline correction was even needless. This was probably due to the relatively simple chemical structure and stable chain conformation of PLLA as well as its defined composition, which induce almost no Raman

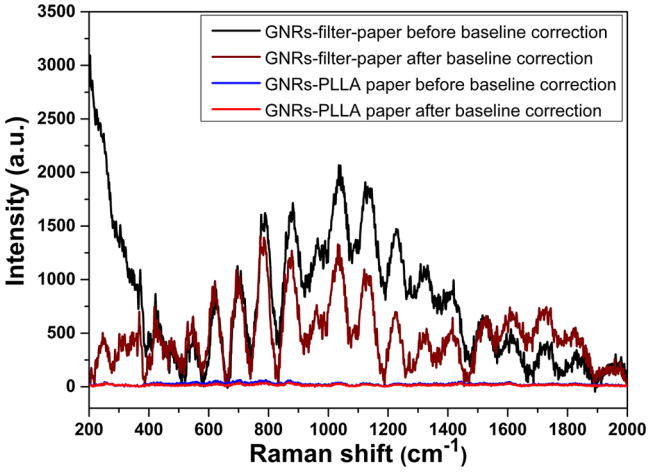

Figure 5. Comparison of background interference between PLLA paper and filter paper coated with GNRs.

signals of the pure PLLA paper (see Supporting Information, Figure S1). It demonstrated the excellent cleanliness of the GNRs-PLLA paper substrate, which could be especially suitable for the detection of trace amount of analyte with faint SERS signal.

The focusing effect of the GNRs-PLLA paper substrate with hydrophobic–hydrophilic partition was investigated by using Rhodamine 6G (R6G) as the typical probe molecules due to its visible color. As shown in Figure 6a–d, when 2 μL of R6G

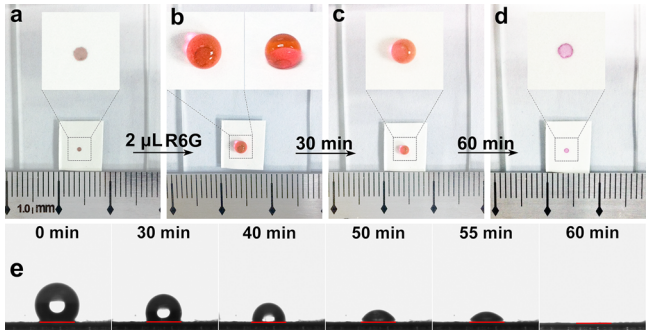

Figure 6. (a–d) Photographs of hydrophobic condensation effect for 2 μL of R6G aqueous solution positioned in the locally hydrophilic hot-spot on the hydrophobic PLLA surface. (e) The side view of this condensation process during evaporation.

aqueous solution was dropped onto the substrate, they were gradually concentrated onto the SERS-active area (covered by the GNRs) during the evaporation process. Figure 6e illustrated the side view of this evaporation process. It was obvious that the contact area (red line) between the R6G droplet and the paper surface was substantially unchanged, which demonstrated the highly efficient concentration of R6G onto the hot-spot in the paper. The patterned substrates with hydrophobic–hydrophilic partition could readily control the transport of liquid, during which the analyte molecules were selectively adhered onto the hydrophilic part.[56,57] Here, only the plasmonic hot-spot area was hydrophilic in such a hydrophobic substrate, thus inducing the hydrophobic–hydrophilic focusing effect that could concentrate the analyte at the small plasmonic hot-spot rather than spreading.

The SERS performance of the GNRs-PLLA paper substrates was further investigated in this study. When 2 μL R6G droplets

DOI: 10.1021/am508881k
ACS Appl. Mater. Interfaces 2015, 7, 5391–5399

at different concentrations were introduced onto the substrate separately, they were concentrated in the hot-spot area due to the aforementioned hydrophobic−hydrophilic focusing effect. After the paper drying, SERS measurements were performed by employing a commercial Raman spectrometer with 633 nm excitation. The experimental process was in a single collection with the exposure time of 10 s. Figure 6a displayed the SERS spectra of R6G with different concentrations varying from 1×10^{-10} to 1×10^{-6} M. From the spectra, the characteristic peaks of R6G at 612, 1360, 1510, and 1650 cm^{-1} could be easily found, which corresponded to one C−C−C ring bending vibration and three aromatic C−C stretching modes, respectively.[58] As illustrated, even at R6G concentrations down to 0.1 nM, the signals could be clearly identified, indicating the excellent SERS enhancement of the GNRs-PLLA paper substrates.

To further demonstrate the SERS performance of GNRs-PLLA paper substrate, the GNRs-filter-paper substrate was selected for comparison (see Figure 7b). Particularly, the SERS signals of R6G in concentration of 1×10^{-6} M could be clearly observed on the GNRs-PLLA paper substrate, whereas very weak signals of R6G in a concentration of 1×10^{-5} M was detected on the GNRs-filter-paper substrate, accompanied by strong background interference from the filter paper. It was believed that the focusing effect contributed greatly to the vastly different SERS performance of these two kinds of papers. For the hydrophilic filter paper, a water droplet of the analyte tended to diffuse over a large area on the paper by capillarity. In terms of the PLLA nanofibrous paper, the hydrophilic SERS-active area served as a concentrator to converge the analyte onto it, thus a greatly improved SERS performance was achieved.

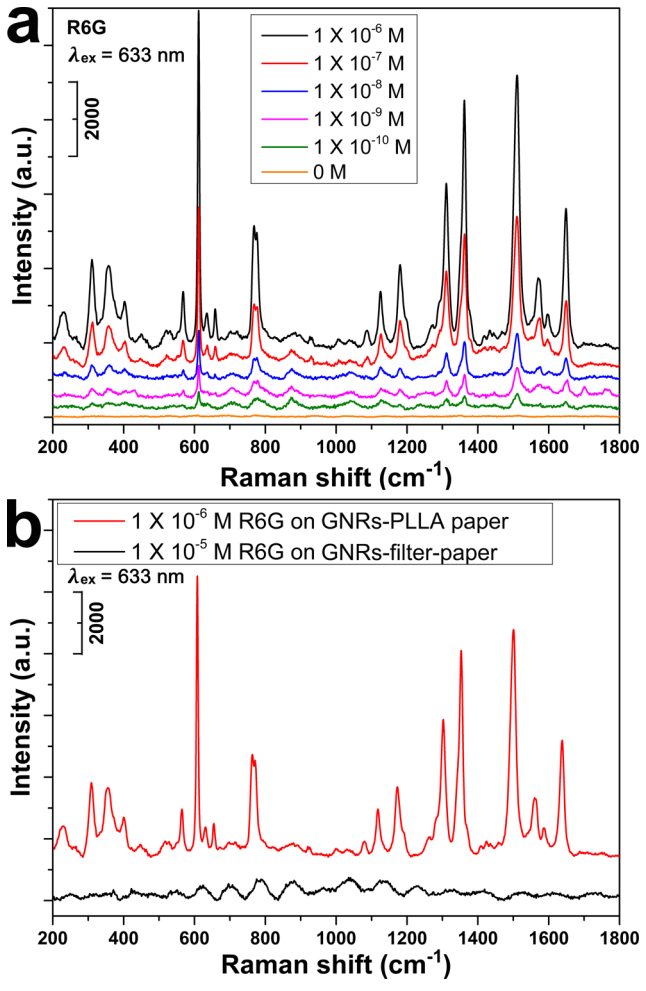

Figure 7. (a) SERS spectra (λ_{ex} = 633 nm) of different concentrations (1×10^{-6} to 1×10^{-10} M) of R6G on GNRs-PLLA paper substrate. (b) SERS spectra comparison of R6G on GNRs-PLLA paper substrate and GNRs-filter-paper substrate.

It was known that the Raman enhancement effect in SERS could be expressed by a value about the enhancement of the Raman signal per molecule adsorbed on an active SERS substrate with respect to the normal Raman signal per molecule.[59] The average enhancement factor (EF) value could be calculated according to the following formula: $EF = (I_{SERS}/N_{SERS})/(I_{Nor}/N_{Nor})$, where I_{SERS} and I_{Nor} are the SERS intensity and normal Raman intensity of the same band of R6G, and N_{SERS} and N_{Nor} represented the corresponding number of molecules probed in the focused incident laser spot. Here in this study, the 612 cm^{-1} band giving the highest peak intensity was selected for such a calculation. On the basis of the calculation method mentioned above, the intensity of the Raman band at 612 cm^{-1} was enhanced by a factor of about 1.08×10^7 (for details, please see the Supporting Information). This Raman enhancement was comparable to the excellent results obtained from the substrates fabricated by advanced nanoengineering processes.[60−62]

We note that the LSPR band of the GNRs influence the Raman enhancement of the substrate. So we chose the short GNRs whose longitudinal SPR band is peaked at 766 nm when they were dispersed in water solution. Furthermore, it is known that the GNR-loaded paper generally exhibits a blue-shifted LSPR band compared to the solution,[24] which can be attributed to the change in the dielectric ambient (from water to air + substrate) with an effective decrease in the refractive index. Here, such a blue-shift can lead to more effective coupling with the 633 nm excitation laser. Although precise measurement of the LSPR band of our substrate is difficult, it is believed that more accurate regulation of the aspect ratio of the original GNRs would further improve the Raman enhancement.

In the next step, the uniformity and reproducibility of GNRs-PLLA substrates was determined. As shown in the SEM image of a typical plasmonic area in Figure 8a, the GNRs on the rim of the area was obviously denser than those in the inner, forming a ring-like shape due to the known "coffee-ring effect".[53] To study the uniformity of the SERS substrate, we registered SERS signals from 13 spots (see Figure 8a) on a single SERS-active area and the data were depicted in Figure 8b,c. It was observed that the SERS signals from the rim spots were higher than those from the inner ones, while the rim spots showed relatively consistent signal intensities for each characteristic band of R6G (Figure 8b). For the strongest peak at 612 cm^{-1}, the relative standard deviation (RSD) of SERS intensities from seven different rim spots on the same substrate was calculated to be about 8% (Figure 8c). In addition, we also tested the intensity variations among different SERS-active areas within an array (Figure 8d). It was obvious that all the SERS-active areas showed relatively consistent signal intensities for each characteristic band of R6G (Figure 8e); the corresponding RSD of SERS intensities at 612 cm^{-1} was about 5% (Figure 8f), indicating a high reproducibility of the GNRs-PLLA paper substrates.

DOI: 10.1021/am508881k
ACS Appl. Mater. Interfaces 2015, 7, 5391−5399

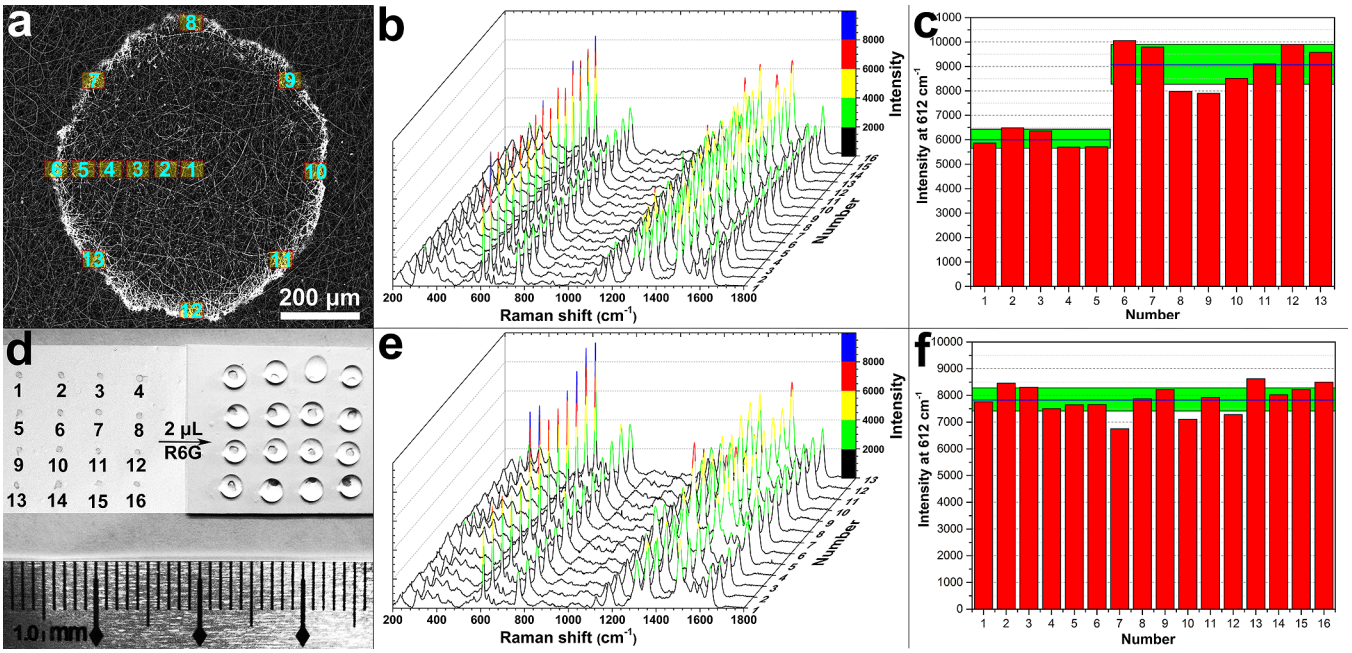

Figure 8. (a) SEM image of a typical SERS-active area. (b,c) SERS spectra of R6G acquired from 13 different spots within a single SERS-active area (b) and the corresponding histogram (c) for the peak intensity at 612 cm^{-1}. (d) Photograph of a SERS array containing 16 SERS-active areas before (left) and after (right) introduction of 2 μL of R6G. (e,f) SERS spectra of R6G acquired from 16 different SERS-active areas within a SERS array (e) and the corresponding histogram (f) for the peak intensity at 612 cm^{-1}.

An ideal substrate should be stable for long-term preservation. In this respect, the stability of the substrate was also studied by comparing the SERS signals from a freshly prepared GNRs-PLLA paper substrate and the substrate after storage in atmospheric conditions for 3 weeks (Figure 9). The results demonstrated that both paper substrates were almost the same in R6G signal intensity, illustrating the long-term stability of GNRs-PLLA paper.

Finally, the applicability of the GNRs-PLLA paper substrates was further investigated by using malachite green as a typical analyte. Malachite green is a kind of shiny metal green crystal belonging to the cationic triphenylmethane dyes, which has been widely used in aquaculture industry and freshwater aquaria as a fungicide and preservative. However, due to the genotoxic and carcinogenic effects, malachite green was banned in several countries and classed under category C.III by FAO/WHO.[63] Hence, it is meaningful to detect trace amounts of MG in water by using a cheap, fast, and sensitive analysis method.[64] In this regard, we employed our SERS substrate in malachite green determination. Figure 10 illustrated the SERS spectra of malachite green in different concentrations varying from 1 × 10^{-6} to 1 × 10^{-10} M. Due to the efficient SERS activity, the spectra clearly showed the characteristic Raman peaks of malachite green: ring C−C stretching (1618 cm^{-1}), *N*-phenyl stretching (1397 cm^{-1}), ring C−H in-plane bending (1172

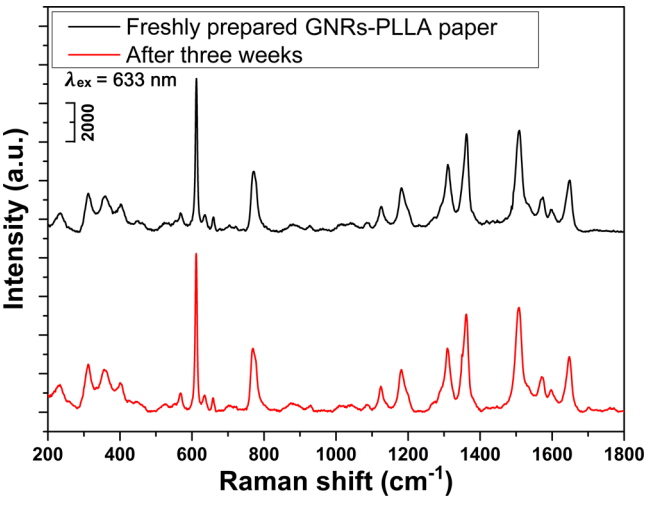

Figure 9. SERS spectra (λ_{ex} = 633 nm) of R6G (1 × 10^{-6} M) acquired from freshly prepared GNRs-PLLA SERS substrate and from a substrate prepared 3 weeks before. Excitation wavelength was 633 nm.

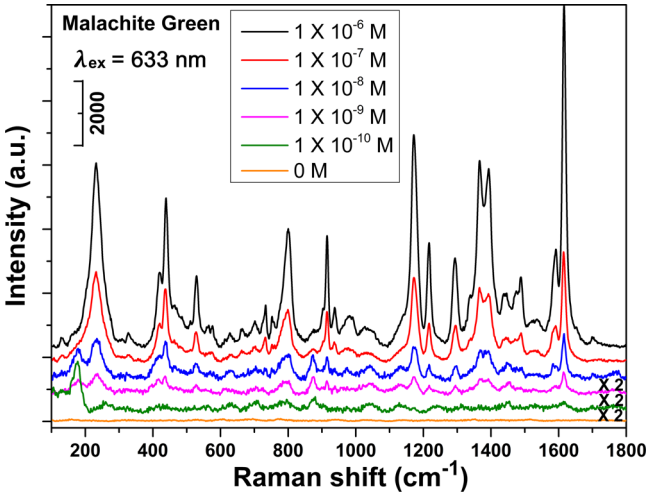

Figure 10. SERS spectra of different concentrations (1 × 10^{-6} to 1 × 10^{-10} M) of malachite green on GNRs-PLLA substrate (the spectra obtained at 1 × 10^{-9} and 1 × 10^{-10} M were amplified 2-fold for clarity).

DOI: 10.1021/am508881k
ACS Appl. Mater. Interfaces 2015, 7, 5391−5399

cm^{-1}), C−H out-of-plane bending (917 and 798 cm^{-1}), and phenyl−C−phenyl out-of-plane bending (438 cm^{-1}).[65] Ascribed from the weak background interference of PLLA paper, SERS signals could be identified clearly even at malachite green concentrations down to 0.1 nM, which indicated that the limit of detection (LOD) was much lower than the method performance limit (2 μg/L) required by the European Commission and the U.S. Food and Drug Administration.[66] It was demonstrated that our SERS substrates could be applicable to the on-site detection of malachite green in practical applications. Moreover, the proposed method made it easily accessible to end-users without complicated fabrication steps.

4. CONCLUSIONS

In summary, we have presented a new paper-based plasmonic SERS substrate with focusing effect by loading GNRs onto PLLA nanofibrous paper. In comparison with the conventional paper substrate, PLLA nanofibrous paper is advanced with extremely clean surface, good hydrophobicity, and negligible background interference under Raman laser excitation. The immobilization of GNRs onto PLLA nanofibrous paper results in a hydrophobic paper substrate with locally hydrophilic SERS-active area, which can confine analyte molecules within it and prevent the random spreading of molecules. With such a focusing effect, the GNRs-PLLA SERS substrate has been found to be highly sensitive in the detection of R6G and malachite green in extremely low concentration (0.1 nM), with excellent reproducibility (~8% RSD) and long-term stability. It is also cost-efficient and does not require tedious fabrication steps. All of these benefits make the obtained PLLA nanofibous paper substrate a really perfect choice for a variety of SERS applications. Furthermore, our results provide an efficient route to enhance the SERS sensitivity by tailoring the hydrophilicity/hydrophobicity of SERS substrate.

■ ASSOCIATED CONTENT

Supporting Information

Raman spectra of PLLA papers and details of the enhancement factor calculation process. This material is available free of charge via the Internet at http://pubs.acs.org.

■ AUTHOR INFORMATION

Corresponding Authors

*E-mail: xf.yu@siat.ac.cn, Tel: 86-755-86392212, Fax: 86-755-86392299 (X.-F.Y.).
*E-mail: hzhang@szu.edu.cn (H.Z.).
*E-mail: duchang@scut.edu.cn (C.D.).

Author Contributions

‖These authors contributed equally to this work.

Notes

The authors declare no competing financial interest.

■ ACKNOWLEDGMENTS

The authors acknowledge financial support from the Natural Science Foundation of China (NSFC) nos. 51372175, 61222505, 61435010, Key grant of Chinese Ministry of Education (313022), Program for Changjiang Scholars and Innovative Research Team in University (IRT 0919), and Guangdong Provincial Program for Excellent Talents in Universities.

■ REFERENCES

(1) Bell, S. E. J.; Sirimuthu, N. M. S. Quantitative Surface-Enhanced Raman Spectroscopy. *Chem. Soc. Rev.* **2008**, *37*, 1012−1024.
(2) Fan, M.; Andrade, G. F. S.; Brolo, A. G. A Review on the Fabrication of Substrates for Surface Enhanced Raman Spectroscopy and their Applications in Analytical Chemistry. *Anal. Chim. Acta* **2011**, *693*, 7−25.
(3) Kneipp, J.; Kneipp, H.; Kneipp, K. SERS—A Single-Molecule and Nanoscale Tool for Bioanalytics. *Chem. Soc. Rev.* **2008**, *37*, 1052−1060.
(4) Ji, W.; Kitahama, Y.; Xue, X.; Zhao, B.; Ozaki, Y. Generation of Pronounced Resonance Profile of Charge-Transfer Contributions to Surface-Enhanced Raman Scattering. *J. Phys. Chem. C* **2012**, *116*, 2515−2520.
(5) Brown, R. J. C.; Milton, M. J. T. Nanostructures and Nanostructured Substrates for Surface-Enhanced Raman Scattering (SERS). *J. Raman Spectrosc.* **2008**, *39*, 1313−1326.
(6) Liu, Y. J.; Chu, H. Y.; Zhao, Y. P. Silver Nanorod Array Substrates Fabricated by Oblique Angle Deposition: Morphological, Optical, and SERS Characterizations. *J. Phys. Chem. C* **2010**, *114*, 8176−8183.
(7) Reilly, T. H.; Corbman, J. D.; Rowlen, K. L. Vapor Deposition Method for Sensitivity Studies on Engineered Surface-Enhanced Raman Scattering-Active Substrates. *Anal. Chem.* **2007**, *79*, 5078−5081.
(8) Yu, Q.; Guan, P.; Qin, D.; Golden, G.; Wallace, P. M. Inverted Size-Dependence of Surface-Enhanced Raman Scattering on Gold Nanohole and Nanodisk Arrays. *Nano Lett.* **2008**, *8*, 1923−1928.
(9) Billot, L.; Lamy de La Chapelle, M.; Grimault, A. S.; Vial, A.; Barchiesi, D.; Bijeon, J.-L.; Adam, P. M.; Royer, P. Surface Enhanced Raman Scattering on Gold Nanowire Arrays: Evidence of Strong Multipolar Surface Plasmon Resonance Enhancement. *Chem. Phys. Lett.* **2006**, *422*, 303−307.
(10) Abu Hatab, N. A.; Oran, J. M.; Sepaniak, M. J. Surface-Enhanced Raman Spectroscopy Substrates Created via Electron Beam Lithography and Nanotransfer Printing. *ACS Nano* **2008**, *2*, 377−385.
(11) Aizpurua, J.; Hanarp, P.; Sutherland, D. S.; Käll, M.; Bryant, G. W.; García de Abajo, F. J. Optical Properties of Gold Nanorings. *Phys. Rev. Lett.* **2003**, *90*, 057401.
(12) Fredriksson, H.; Alaverdyan, Y.; Dmitriev, A.; Langhammer, C.; Sutherland, D. S.; Zäch, M.; Kasemo, B. Hole−Mask Colloidal Lithography. *Adv. Mater.* **2007**, *19*, 4297−4302.
(13) Haynes, C. L.; Van Duyne, R. P. Nanosphere Lithography: A Versatile Nanofabrication Tool for Studies of Size-Dependent Nanoparticle Optics. *J. Phys. Chem. B* **2001**, *105*, 5599−5611.
(14) McFarland, A. D.; Young, M. A.; Dieringer, J. A.; Van Duyne, R. P. Wavelength-Scanned Surface-Enhanced Raman Excitation Spectroscopy. *J. Phys. Chem. B* **2005**, *109*, 11279−11285.
(15) Tripp, R. A.; Dluhy, R. A.; Zhao, Y. Novel Nanostructures for SERS Biosensing. *Nano Today* **2008**, *3*, 31−37.
(16) Cheng, C.; Yan, B.; Wong, S. M.; Li, X.; Zhou, W.; Yu, T.; Shen, Z.; Yu, H.; Fan, H. J. Fabrication and SERS Performance of Silver-Nanoparticle-Decorated Si/ZnO Nanotrees in Ordered Arrays. *ACS Appl. Mater. Interfaces* **2010**, *2*, 1824−1828.
(17) He, D.; Hu, B.; Yao, Q. F.; Wang, K.; Yu, S. H. Large-Scale Synthesis of Flexible Free-Standing SERS Substrates with High Sensitivity: Electrospun PVA Nanofibers Embedded with Controlled Alignment of Silver Nanoparticles. *ACS Nano* **2009**, *3*, 3993−4002.
(18) Ahmed, A.; Gordon, R. Single Molecule Directivity Enhanced Raman Scattering using Nanoantennas. *Nano Lett.* **2012**, *12*, 2625−2630.
(19) Betz, J. F.; Wei, W. Y.; Cheng, Y.; White, I. M.; Rubloff, G. W. Simple SERS Substrates: Powerful, Portable, and Full of Potential. *Phys. Chem. Chem. Phys.* **2014**, *16*, 2224−2239.
(20) Araújo, A.; Caro, C.; Mendes, M. J.; Nunes, D.; Fortunato, E.; Franco, R.; Águas, H.; Martins, R. Highly Efficient Nanoplasmonic SERS on Cardboard Packaging Substrates. *Nanotechnology* **2014**, *25*, 415202.

DOI: 10.1021/am508881k
ACS Appl. Mater. Interfaces 2015, 7, 5391−5399

(21) Zhang, W.; Li, B.; Chen, L.; Wang, Y.; Gao, D.; Ma, X.; Wu, A. Brushing, a Simple Way to Fabricate SERS Active Paper Substrates. *Anal. Methods* **2014**, *6*, 2066−2071.
(22) Abbas, A.; Brimer, A.; Slocik, J. M.; Tian, L.; Naik, R. R.; Singamaneni, S. Multifunctional Analytical Platform on a Paper Strip: Separation, Preconcentration, and Subattomolar Detection. *Anal. Chem.* **2013**, *85*, 3977−3983.
(23) Qu, L. L.; Li, D. W.; Xue, J. Q.; Zhai, W. L.; Fossey, J. S.; Long, Y. T. Batch Fabrication of Disposable Screen Printed SERS Arrays. *Lab Chip* **2012**, *12*, 876−881.
(24) Lee, C. H.; Tian, L.; Singamaneni, S. Paper-Based SERS Swab for Rapid Ttrace Detection on Real-World Surfaces. *ACS Appl. Mater. Interfaces* **2010**, *2*, 3429−3435.
(25) Ngo, Y. H.; Li, D.; Simon, G. P.; Garnier, G. Gold Nanoparticle-Paper as a Three-Dimensional Surface Enhanced Raman Scattering Substrate. *Langmuir* **2012**, *28*, 8782−8790.
(26) Chen, Y.; Cheng, H.; Tram, K.; Zhang, S.; Zhao, Y.; Han, L.; Chen, Z.; Huan, S. A Paper-Based Surface-Enhanced Resonance Raman Spectroscopic (SERRS) Immunoassay Using Magnetic Separation and Enzyme-Catalyzed Reaction. *Analyst* **2013**, *138*, 2624−2631.
(27) Polavarapu, L.; Porta, A. L.; Novikov, S. M.; Coronado-Puchau, M.; Liz-Marzán, L. M. Pen-on-Paper Approach Toward the Design of Universal Surface Enhanced Raman Scattering Substrates. *Small* **2014**, *10*, 3065.
(28) Wei, W. Y.; White, I. M. Chromatographic Separation and Detection of Target Analytes from Complex Samples Using Inkjet Printed SERS Substrates. *Analyst* **2013**, *138*, 3679−3686.
(29) Yu, W. W.; White, I. M. Inkjet Printed Surface Enhanced Raman Spectroscopy Array on Cellulose Paper. *Anal. Chem.* **2010**, *82*, 9626−9630.
(30) Polavarapu, L.; Liz-Marzán, L. M. Towards Low-cost Flexible Substrates for Nanoplasmonic Sensing. *Phys. Chem. Chem. Phys.* **2013**, *15*, 5288−5300.
(31) De Angelis, F.; Gentile, F.; Mecarini, F.; Das, G.; Moretti, M.; Candeloro, P.; Coluccio, M. L.; Cojoc, G.; Accardo, A.; Liberale, C.; Zaccaria, R. P.; Perozziello, G.; Tirinato, L.; Toma, A.; Cuda, G.; Cingolani, R.; Di Fabrizio, E. Breaking the Diffusion Limit with Super-Hydrophobic Delivery of Molecules to Plasmonic Nanofocusing SERS Structures. *Nature Photonics* **2011**, *5*, 682−687.
(32) Lu, L. Q.; Zheng, Y.; Qu, W. G.; Yu, H. Q.; Xu, A. W. Hydrophobic Teflon Films as Concentrators for Single-Molecule SERS Detection. *J. Mater. Chem.* **2012**, *22*, 20986−20990.
(33) Hu, J.; Sun, X.; Ma, H.; Xie, C.; Chen, Y. E.; Ma, P. X. Porous Nanofibrous PLLA Scaffolds for Vascular Tissue Engineering. *Biomaterials* **2010**, *31*, 7971−7977.
(34) Shao, J.; Wang, Y.; Chen, X.; Hu, X.; Du, C. Nanomechanical Properties of Poly (L-lactide) Nanofibers after Deformation. *Colloids Surf., B* **2014**, *120*, 97−101.
(35) Maharana, T.; Mohanty, B.; Negi, Y. S. Melt-Solid Polycondensation of Lactic Acid and its Biodegradability. *Prog. Polym. Sci.* **2009**, *34*, 99−124.
(36) Yang, F.; Murugan, R.; Wang, S.; Ramakrishna, S. Electrospinning of Nano/micro Scale Poly (L-lactic acid) Aligned Fibers and their Potential in Neural Tissue Engineering. *Biomaterials* **2005**, *26*, 2603−2610.
(37) Wang, J. H.; Wang, B.; Liu, Q.; Li, Q.; Huang, H.; Song, L.; Sun, T. Y.; Wang, H. Y.; Yu, X. F.; Li, C. Z.; Chu, P. K. Bimodal Optical Diagnostics of Oral Cancer Based on Rose Bengal Conjugated Gold Nanorod Platform. *Biomaterials* **2013**, *34*, 4274−4283.
(38) Orendorff, C. J.; Murphy, C. J. Quantitation of Metal Content in the Silver-Assisted Growth of Gold Nanorods. *J. Phys. Chem. B* **2006**, *110*, 3990−3994.
(39) Chen, J. P.; Su, C. H. Surface Modification of Electrospun PLLA Nanofibers by Plasma Treatment and Cationized Gelatin Immobilization for Cartilage Tissue Engineering. *Acta Biomater.* **2011**, *7*, 234−243.
(40) Chakraborty, S.; Liao, I.; Adler, A.; Leong, K. W. Electrohydrodynamics: A Facile Technique to Fabricate Drug Delivery Systems. *Adv. Drug Delivery Rev.* **2009**, *61*, 1043−1054.
(41) Shao, J.; Chen, C.; Wang, Y.; Chen, X.; Du, C. Early Stage Structural Evolution of PLLA Porous Scaffolds in Thermally Induced Phase Separation Process and the Corresponding Biodegradability and Biological Property. *Polym. Degrad. Stab.* **2012**, *97*, 955−963.
(42) von Maltzahn, G.; Centrone, A.; Park, J. H.; Ramanathan, R.; Sailor, M. J. SERS-Coded Gold Nanorods as a Multifunctional Platform for Densely Multiplexed Near-Infrared Imaging and Photothermal Heating. *Adv. Mater.* **2009**, *21*, 3175−3180.
(43) Jokerst, J. V.; Cole, A. J.; Van de Sompel, D.; Gambhir, S. S. Gold Nanorods for Ovarian Cancer Detection with Photoacoustic Imaging and Resection Guidance via Raman Imaging in Living Mice. *ACS Nano* **2012**, *6*, 10366−10377.
(44) Ni, W.; Kou, X.; Yang, Z.; Wang, J. F. Tailoring Longitudinal Surface Plasmon Wavelengths, Scattering and Absorption Cross Sections of Gold Nanorods. *ACS Nano* **2008**, *2*, 677−686.
(45) Huang, H.; Wang, J. H.; Jin, W.; Li, P.; Chen, M.; Xie, H. H.; Yu, X. F.; Wang, H.; Dai, Z.; Xiao, X.; Chu, P. K. Competitive Reaction Pathway for Site-Selective Conjugation of Raman Dyes to Hotspots on Gold Nanorods for Greatly Enhanced SERS Performance. *Small* **2014**, *10*, 4012−4019.
(46) Peng, B.; Li, G.; Li, D.; Dodson, S.; Zhang, Q.; Zhang, J.; Lee, Y. H.; Demir, H. V.; Ling, X. Y.; Xiong, Q. Vertically Aligned Gold Nanorod Monolayer on Arbitrary Substrates: Self-Assembly and Femtomolar Detection of Food Contaminants. *ACS Nano* **2013**, *7*, 5993−6000.
(47) Chen, H.; Ming, T.; Zhao, L.; Wang, F.; Sun, L. D.; Wang, J.; Yan, C. H. Plasmon−Molecule Interactions. *Nano Today* **2010**, *5*, 494−505.
(48) Liu, Q.; Wang, J.; Wang, B.; Li, Z.; Huang, H.; Li, C.; Yu, X. F.; Chu, P. K. Paper-Based Plasmonic Platform for Sensitive, Noninvasive, and Rapid Cancer Screening. *Biosens. Bioelectron.* **2014**, *54*, 128−134.
(49) Dai, Z.; Xiao, X.; Wu, W.; Liao, L.; Mei, F.; Yu, X.; Guo, S.; Ying, J.; Reng, F.; Jiang, C. Side-to-Side Alignment of Gold Nanorods with Polarization-Free Characteristic for Highly Reproducible Surface Enhanced Raman Scattering. *Appl. Phys. Lett.* **2014**, *105*, 211902.
(50) Chen, H.; Shao, L.; Li, Q.; Wang, J. Gold Nanorods and Their Plasmonic Properties. *Chem. Soc. Rev.* **2013**, *42*, 2679−2724.
(51) Huang, X.; Neretina, S.; El-Sayed, M. A. Gold Nanorods: From Synthesis and Properties to Biological and Biomedical Applications. *Adv. Mater.* **2009**, *21*, 4880−4910.
(52) Hu, F. X.; Neoh, K. G.; Kang, E. T. Synthesis and in Vitro Anti-Cancer Evaluation of Tamoxifen-Loaded Magnetite/PLLA Composite Nanoparticles. *Biomaterials* **2006**, *27*, 5725−5733.
(53) Halvorson, R. A.; Vikesland, P. J. Drop Coating Deposition Raman (DCDR) for Microcystin-LR Identification and Quantitation. *Environ. Sci. Technol.* **2011**, *45*, 5644−5651.
(54) Tang, W.; Chase, D. B.; Rabolt, J. F. Immobilization of Gold Nanorods onto Electrospun Polycaprolactone Fibers via Polyelectrolyte Decoration—A 3D SERS Substrate. *Anal. Chem.* **2013**, *85*, 10702−10709.
(55) Dong, X. M.; Revol, J.; Gray, D. G. Effect of Microcrystallite Preparation Conditions on the Formation of Colloid Crystals of Cellulose. *Cellulose* **1998**, *5*, 19−32.
(56) Li, X.; Tian, J.; Nguyen, T.; Shen, W. Paper-Based Microfluidic Devices by Plasma Treatment. *Anal. Chem.* **2008**, *80*, 9131−9134.
(57) Ahmed, W.; Glass, C.; Kooij, E. S.; van Ruitenbeek, J. M. Tuning the Oriented Deposition of Gold Nanorods on Patterned Substrates. *Nanotechnology* **2014**, *25*, 035301.
(58) Hildebrandt, P.; Stockburger, M. Surface-Enhanced Resonance Raman Spectroscopy of Rhodamine 6G Adsorbed on Colloidal Silver. *J. Phys. Chem.* **1984**, *88*, 5935−5944.
(59) Stamplecoskie, K. G.; Scaiano, J. C.; Tiwari, V. S.; Anis, H. Optimal Size of Silver Nanoparticles for Surface-Enhanced Raman Spectroscopy. *J. Phys. Chem. C* **2011**, *115*, 1403−1409.

DOI: 10.1021/am508881k
ACS Appl. Mater. Interfaces 2015, 7, 5391−5399

(60) Liu, J.; White, I.; DeVoe, D. L. Nanoparticle-Functionalized Porous Polymer Monolith Detection Elements for Surface-Enhanced Raman Scattering. *Anal. Chem.* **2011**, *83*, 2119−2124.
(61) Mai, F. D.; Hsu, T. C.; Liu, Y. C.; Yang, K. H.; Chen, B. C. A New Strategy to Prepare Surface-Enhanced Raman Scattering-Active Substrates by Electrochemical Pulse Deposition of Gold Nanoparticles. *Chem. Commun.* **2011**, *47*, 2958−2960.
(62) Rajapandiyan, P.; Yang, J. Photochemical Method for Decoration of Silver Nanoparticles on Filter Paper Substrate for SERS Application. *J. Raman Spectrosc.* **2014**, *45*, 574−580.
(63) Bose, B.; Motiwale, L.; Rao, K. V. K. DNA Damage and G2/M Arrest in Syrian Hamster Embryo Cells During Malachite Green Exposure are Associated with Elevated Phosphorylation of ERK1 and JNK1. *Cancer Lett.* **2005**, *230*, 260−270.
(64) Lee, S.; Choi, J.; Chen, L.; Park, B.; Kyong, J. B.; Seong, G. H.; Choo, J.; Lee, Y.; Shin, K. H.; Lee, E. K.; Joo, S. W.; Lee, K. H. Fast and Sensitive Trace Analysis of Malachite Green Using a Surface-Enhanced Raman Microfluidic Sensor. *Anal. Chim. Acta* **2007**, *590*, 139−144.
(65) Zhang, Y.; Yu, W.; Pei, L.; Lai, K.; Rasco, B. A.; Huang, Y. Rapid Analysis of Malachite Green and Leucomalachite Green in Fish Muscles with Surface-Enhanced Resonance Raman Scattering. *Food Chem.* **2015**, *169*, 80−84.
(66) Quang, L. X.; Lim, C.; Seong, G. H.; Choo, J.; Do, K. J.; Yoo, S. K. A Portable Surface-Enhanced Raman Scattering Sensor Integrated with a Lab-on-a-Chip for Field Analysis. *Lab Chip* **2008**, *8*, 2214−2219.

DOI: 10.1021/am508881k
ACS Appl. Mater. Interfaces 2015, 7, 5391−5399